

Electron Paramagnetic Resonance of Copper in Beryllium Oxide*

M. DE WIT AND A. R. REINBERG
Texas Instruments Incorporated, Dallas, Texas

(Received 21 June 1967)

Paramagnetic-resonance absorption of copper-doped single crystals of beryllium oxide has been investigated at 9 GHz. The best-fit values to a spin Hamiltonian with $S = \frac{1}{2}$ are $|g_{||}| = 1.709 \pm 0.002$, $|g_{\perp}| = 2.379 \pm 0.001$, $|A_{||}| = (50 \pm 1) \times 10^{-4} \text{ cm}^{-1}$, $|A_{\perp}| = (108 \pm 1) \times 10^{-4} \text{ cm}^{-1}$, and $|Q| = (11 \pm 1) \times 10^{-4} \text{ cm}^{-1}$, where the hyperfine values refer to the Cu^{63} isotope, for which $I = \frac{3}{2}$. The observations are interpreted as due to Cu^{2+} substitutional for beryllium at normal lattice sites. Crystal-field theory which incorporates covalent bonding has been used to interpret these results in terms of the $3d^9$ configuration of Cu^{2+} in C_{3v} symmetry. The experimental results are shown to be consistent with the theory, which yields an orbital reduction factor of 0.6, and values for $\langle r^{-3} \rangle$ and the contact hyperfine interaction close to those for the free ion. The results are also compared with some other cases of $3d^9$ ions in tetrahedral coordination.

INTRODUCTION

COPPER is important as an activator of luminescence and plays a role in determining the optical and electrical properties of a number of tetrahedrally coordinated II-VI compounds. Although the subject of many investigations, these materials containing copper as an impurity have only recently been extensively studied by the technique of electron paramagnetic resonance (EPR).¹ In this paper we report on an investigation by EPR of copper-doped single crystals of BeO. While not directly considered to be a II-VI compound in the sense of the series Zn or Cd with O, S, Se, and Te, BeO crystallizes in the wurtzite lattice making it an interesting comparison to the isomorphous compounds ZnO and CdS. Copper in ZnO has been studied in great detail by Dietz, Kamimura, Sturge, and Yariv² by both optical and EPR techniques, while less complete EPR³ and optical⁴ results are known for CdS. The complex nature of the $3d^9$ Cu^{2+} configuration in tetrahedral coordination is indicated by the wide diversity of results that have been observed.¹

We have attempted an explanation of the EPR results for copper in BeO by assuming that $3d^9$ Cu^{2+} substitutes for beryllium in an axially distorted tetrahedral crystal field. By applying the method of Dietz *et al.*² of crystal-field theory incorporating covalent bonding, our observations are found to be consistent with an orbital reduction factor of 0.6 together with a strong axial field. Attempts to obtain the positions of the higher-lying states by optical absorption were unsuccessful, so that at least one of the two second-order terms required had to be assumed. The quantitative fit to the observations is very good and it is found that the expectation values of r^{-3} and the net spin density at

the nucleus are close to the free-ion values when the $\text{Cu}^{2+}\text{-O}^{2-}$ overlap matrix element is taken near that for the free ions. These results may be compared with those for the ZnO:Cu system, where a complete fit using excited-state data shows large differences from the free-ion values.

Even though the fit of the theory to the BeO:Cu case appears good, additional information about this system could modify it. At best, we show the results consistent with the theory but we are not able to rule out other explanations of the observations.

EXPERIMENT

The single crystals used in this investigation were generously supplied by S. B. Austerman of Atomics International.⁵ They were usually in the form of small prisms or pyramids with excellent morphology which allowed crude orientation of the crystal axes to be made visually. The crystals, which were grown from lithium molybdate flux, were quite pure as received, containing only small amounts of B, Si, Mg, and less than 1 ppm Cu as determined by emission spectrographic analysis. No EPR signals were observed in undoped crystals unless they were irradiated with x rays. Copper was introduced into the crystals by diffusion from the molten metal by placing the crystals in a graphite crucible along with either pure copper metal or cuprous oxide and heating it to temperatures ranging from 1300 to 1700°C for periods of 24–80 h. This treatment usually resulted in severe attack of the crystal surfaces, making it difficult to prepare good optical quality samples. EPR signals which are attributed to copper were observed in most of the diffused samples without any additional treatment such as x irradiation. Irradiation with 50 kV x rays either at room or at low temperature did not affect the copper signals but did produce other signals such as boron donors.⁶ Most of the data were taken with unirradiated crystals because the irradiation produced signals which tended to mask the copper resonance.

⁵ S. B. Austerman, J. Nucl. Materials 14, 225 (1964), and references therein for growth methods and properties.

⁶ A. R. Reinberg, J. Chem. Phys. 41, 850 (1964).

* Work sponsored in part by the U.S. Air Force Office of Scientific Research under Contract No. F44620-67-C-0073.

¹ T. L. Estle, W. C. Holton, M. de Wit, R. K. Watts, A. R. Reinberg, and J. Schneider, in *Proceedings of the International Conference on Luminescence*, Budapest, 1966 (to be published).

² R. E. Dietz, H. Kamimura, M. D. Sturge, and A. Yariv, Phys. Rev. 132, 1559 (1963), hereafter referred to as DKSY.

³ K. Morigaki, J. Phys. Soc. Japan 19, 1240 (1964).

⁴ I. Broser, H. Maier, and H.-J. Schultz, Phys. Rev. 140, A2135 (1965).

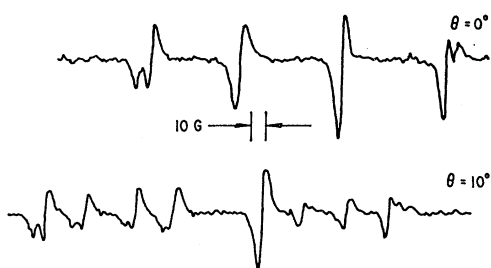


FIG. 1. Paramagnetic resonance spectrum of BeO:Cu, with the external field along crystal c axis, $\theta=0^\circ$ and 10° from the c axis.

The X-band EPR spectrometer employed in this investigation was of conventional design, utilizing superheterodyne detection. For accurate angular-dependence measurements, the samples were placed on a rotating Teflon post within the microwave cavity whose axis was perpendicular to the axis about which the magnet was rotated. Temperature measurements were made by placing a copper-constantan thermocouple in contact with the sample in such a way that the thermocouple leads were along the axis of the TE_{011} cylindrical mode cavity employed.

RESULTS

EPR spectra showing well-resolved copper hyperfine structure (hfs) were observed from 1.3 to $\sim 30^\circ\text{K}$. At the lowest temperatures, the signals were readily saturated and could only be observed at microwave power levels of -50 dBm and below. A typical spectrum for the case where the magnetic field is parallel to the crystal c axis is shown in Fig. 1. Both the Cu^{63} and the Cu^{65} isotopes are clearly resolved. The relative splitting and the intensities of the outermost sets of lines are consistent with what is to be expected for the copper isotopes based on known values of their nuclear magnetic moments and relative abundance. This, together with the absence of signals in samples that have not been diffused in copper, is taken to be proof that we are observing EPR signals due to copper. A striking feature of the spectrum is the appearance of strong "forbidden" transitions when the magnetic field is rotated away from the crystal c axis. A typical spectrum for an orientation near the c axis is also shown in Fig. 1. Only a single copper spectrum is observed, and it has axial symmetry with the crystal c axis as the principal direction.

The observed angular dependence at 1.3°K has been fitted to a spin Hamiltonian⁷

$$\mathcal{H} = \beta \mathbf{H} \cdot \mathbf{g} \cdot \mathbf{S} + \mathbf{I} \cdot \mathbf{A} \cdot \mathbf{S} + Q [I_z^2 - \frac{1}{3} I(I+1)], \quad (1)$$

where β is the Bohr magneton. The spin quantum numbers are $S = \frac{1}{2}$ and $I = \frac{3}{2}$, with the z direction along the crystal c axis. The tensors \mathbf{g} and \mathbf{A} have two principal

⁷ A. Abragam and M. H. L. Pryce, Proc. Roy. Soc. (London) **A205**, 135 (1951).

values, as required for axial symmetry. The best values of Q , the quadrupole coupling constant, were obtained by a computer fit to the small-angle data for the "forbidden" transitions. The results for Cu^{63} are $|g_{\parallel}| = 1.709 \pm 0.002$, $|g_{\perp}| = 2.379 \pm 0.001$, $|A_{\parallel}| = (50 \pm 1) \times 10^{-4} \text{ cm}^{-1}$, $|A_{\perp}| = (108 \pm 1) \times 10^{-4} \text{ cm}^{-1}$, and $|Q| = (11 \pm 1) \times 10^{-4} \text{ cm}^{-1}$. The quality of the fit is well illustrated in Fig. 2, where the predicted angular dependence generated from a computer calculation is compared with the experimental data points. The calculated intensity ratio between allowed and forbidden transitions is 2:1 at $\theta = 10^\circ$, compared with 4:3 as shown in Fig. 1. The difficulty in measuring the intensities is compounded by the two isotopes and the low signal-to-noise ratio and recording almost under fast-passage conditions. These observations therefore do not detract from the quality of the fit. A second feature of the forbidden transitions is that they appear to merge with the allowed lines at $\theta = 0^\circ$. This is a consequence of the fact that $|A_{\parallel}|/Q \simeq 4$.

Since no spectra could be seen at 77°K , an attempt was made to examine the temperature dependence. Qualitatively, the relaxation time was observed to decrease only slightly from 1.3 to 4.2°K but by 14°K had decreased sufficiently so that spectra could be observed with 40 dB more power than could be used at 4.2°K . Detailed saturation data could not be obtained because of the weak signals, so that the actual change in relaxation time is not known. At somewhat higher temperatures the linewidth increases and the line continues to broaden until it becomes unobservable at about 31°K . It was not possible to determine unambiguously the functional form of the temperature dependence of the relaxation time by this method. Exponential, T^{-7} , and T^{-9} dependences all gave reasonably good fits to the experimental data. If,

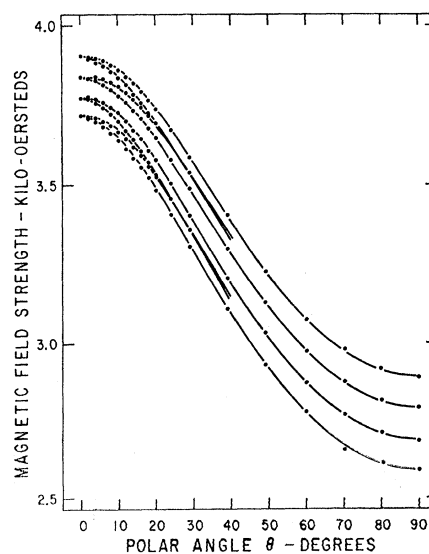


FIG. 2. Angular dependence of the EPR spectrum.

however, one assumes a temperature dependence $\exp\Delta/kT$, as would result from an Orbach relaxation,⁸ a value of $\Delta = 30 \text{ cm}^{-1}$ is obtained. However, no detailed study of the line shape was possible because of the low copper concentration and consequent low signal-to-noise ratio. A similar experiment was made on ZnO:Cu and yielded a value $\Delta = 60 \text{ cm}^{-1}$. This might be compared with the splitting between the two lowest Γ_6 levels of 123 cm^{-1} as reported by Dietz *et al.*² from their optical studies. The results are, however, ambiguous and were therefore not used in the theoretical analysis.

Although it is reasonably certain that we are observing EPR signals due to copper, the configuration of the copper defect needs to be examined further. First we must consider the charge state and possible sites into which a copper impurity might go. Since only the neutral copper atom Cu^0 and the double positively charged ion Cu^{2+} will have unpaired electron spins, we need reasonably only consider the possibilities of Cu^0 in interstitial positions and Cu^{2+} ions substitutionally located on beryllium sites. Another possibility which cannot be discarded with complete certainty is that of the positively charged ion in an interstitial site associated with a local charge-compensating defect such as a beryllium vacancy. The observation of only a center with c -axis symmetry requires that such a compensating defect would only be in the direction of the crystal c axis away from the copper impurity. Although this does not seem very likely, it can not be completely eliminated as a possibility, particularly in light of the large polar electric field that exists in BeO. With respect to neutral copper, the expected hyperfine splitting for its $^2S_{1/2}$ ground state is 2425 Oe , as deduced from atomic-beam measurements on isolated copper atoms⁹ and would, furthermore, be nearly isotropic leaving only substitutional Cu^{2+} as a reasonable configuration. In the following discussions we will examine some consequences of the assumption that the EPR signals are due to simple isolated Cu^{2+} substituting for beryllium at normal lattice sites. The C_{3v} symmetry at this site is that of an axially distorted tetrahedron of negative charges.

ANALYSIS

A theoretical analysis for the $3d^9$ configuration in C_{3v} symmetry has been given by DKSY and also by Bates.¹⁰ An effective Hamiltonian determined from the symmetry according to Tanabe and Kamimura¹¹ was constructed. Effects of covalency were also included and the problem was solved in considerable detail. We shall review briefly the energy-level structure and wave function for this problem and quote the relevant formulas used.

⁸ R. Orbach, Proc. Roy. Soc. (London) **A264**, 458 (1961).

⁹ Y. Ting and H. Lew, Phys. Rev. **105**, 581 (1957).

¹⁰ C. A. Bates, Proc. Phys. Soc. (London) **83**, 465 (1964).

¹¹ Y. Tanabe and H. Kamimura, J. Phys. Soc. Japan **13**, 394 (1958).

When placed in a site of tetrahedral symmetry, the electronic d function reduces to the representations t_2 and e of the group T_d . The $3d^9$ configuration may be considered as a hole in an otherwise filled $3d^{10}$ shell. In the case of the metal substitutional site in II-VI compounds, the single $3d$ hole configuration has as its lowest state the t_2 configuration and the e configuration is an amount $10 Dq$ higher in energy. These configurations lead to the terms 2T_2 and 2E , respectively. When the symmetry is reduced to C_{3v} and the spin-orbit interaction is taken into account, the 2T_2 term of T_d symmetry reduces to the representations $2\Gamma_6 + \Gamma_{4,5}$ of C_{3v} symmetry with a Γ_6 term lowest. Similarly, the term 2E reduces to $\Gamma_6 + \Gamma_{4,5}$. Here Γ_6 and $\Gamma_{4,5}$ are Kramer's doublets. The paramagnetic resonance results are all obtained from the lowest energy state and the $\Gamma_{4,5}$ states are not considered further. A 3×3 Hamiltonian matrix for the Γ_6 states is readily computed. We use the eigenfunctions for tetrahedral symmetry with the quantization axis along the $[111]$ direction as a basis:

$$\begin{aligned} |\Gamma_6^1, \pm\rangle &= \{\varphi_0\chi_{\pm 1/2} - \sqrt{2}\varphi_{\pm 1}\chi_{\mp 1/2}\}/\sqrt{3}, \\ |\Gamma_6^2, \pm\rangle &= -\{\sqrt{2}\varphi_0\chi_{\pm 1/2} + \varphi_{\pm 1}\chi_{\mp 1/2}\}/\sqrt{3}, \end{aligned} \quad (2)$$

for the t_2 configuration. For the e configuration,

$$|\Gamma_6, \pm\rangle = \psi_{\pm 1}\chi_{\mp 1/2}. \quad (3)$$

The $\chi_{\pm 1/2}$ are the spin functions and the angular parts of the basis functions are defined in terms of the spherical harmonics $Y_{l,m}$ as

$$\begin{aligned} \varphi_0 &= -Y_{2,0}R_{l_2}, \\ \varphi_1 &= -\varphi_{-1}^* = (Y_{2,1} + \sqrt{2}Y_{2,-2})R_{l_2}/\sqrt{3}, \\ \psi_1 &= -\psi_{-1}^* = (\sqrt{2}Y_{2,1} - Y_{2,-2})R_e/\sqrt{3}, \end{aligned} \quad (4)$$

where R_{l_2} and R_e are the radial parts of the functions. In addition, the $3d$ electrons on the Cu ion may take part in the bonding to the neighboring oxygen atoms in the lattice. For T_d symmetry both σ - and π -like orbitals may be admixed into the t_2 functions but only π admixture is allowed with the e functions. The π admixtures are expected to be very small in covalent hosts,² and we also omit them in BeO in order to simplify the calculation. Instead of the orbitals φ_m we use the linear-combination-of-atomic-orbitals molecular orbitals

$$\begin{aligned} \Phi_m &= N\{\varphi_m - \eta\sigma_l\}, \\ N^2 &= (1 - 4\eta S + \eta^2)^{-1}, \end{aligned} \quad (5)$$

where N is a renormalization factor, S is the overlap integral between the function φ and a σ orbital on a particular oxygen, while η is the admixture coefficient and σ_l is a normalized linear combination of orbitals on the nearest ligand oxygen ions with the appropriate σ symmetry. The effect of using the Φ_m is to modify the matrix elements of the orbital Zeeman effect by

the orbital reduction factor k^{12} :

$$\langle \varphi_m | L_i | \varphi_{m'} \rangle = k \langle \Phi_m | L_i | \Phi_{m'} \rangle, \quad k = 1 - \eta^2 N^2, \quad (6)$$

and also to introduce a factor N or N^2 in other matrix elements. A similar reduction factor for the matrix elements of L_i between the t_2 and e configurations is taken to be unity. The ligand π -function admixture is neglected and therefore the modification of the spin-orbit interaction on the central ion by that on the ligands¹³ is small and may be neglected, because the spin-orbit interaction of the σ functions on each neighbor vanishes.

The ground-state wave function is a linear combination of the functions (2) and (3) modified for covalency effects as in (5):

$$| \Gamma_6^g, m \rangle = a | \Gamma_6^1, m \rangle + b | \Gamma_6^2, m \rangle + c | \Gamma_6, m \rangle. \quad (7)$$

The expressions for the spin-Hamiltonian parameters are then, to order c ,

$$\begin{aligned} g_{||} &= -\frac{2}{3}(2k+1)a^2 - \frac{2}{3}(k-1)b^2 - 4\sqrt{2}(k+2)ab/3 \\ &\quad - 8ac/\sqrt{3} - 4\sqrt{2}bc/\sqrt{3}, \\ g_{\perp} &= \frac{2}{3}(2k+1)a^2 - \frac{4}{3}(k-1)b^2 - 2\sqrt{2}(k+2)ab/3 \\ &\quad - 4ac/\sqrt{3} + 4\sqrt{2}bc/\sqrt{3}, \\ A_{||} &= N^2 P [-2\chi(a^2 - b^2 + 4\sqrt{2}ab)/9 \\ &\quad - \langle r^{-3} \rangle (8a^2 + 10\sqrt{2}ab)/7] \\ &\quad - NP \langle r^{-3} \rangle' (44ac/7\sqrt{3} + 4\sqrt{2}bc/\sqrt{3}), \\ A_{\perp} &= -N^2 P [-2\chi(a^2 + 2b^2 - 2\sqrt{2}ab)/9 \\ &\quad + \langle r^{-3} \rangle (-8a^2 + 12b^2 + 5\sqrt{2}ab)/7] \\ &\quad - NP \langle r^{-3} \rangle' (22ac - 34\sqrt{2}bc)/7\sqrt{3}, \\ Q &= -N^2 Q_0 \langle r^{-3} \rangle (-2\sqrt{2}ab + b^2) \\ &\quad + N Q_0 \langle r^{-3} \rangle' (4ac + 2\sqrt{2}bc)/\sqrt{3}, \quad (8) \end{aligned}$$

where $P = 2\beta\beta_n\mu/Ia_0^3 = 47.11 \times 10^{-4} \text{ cm}^{-1}/\text{a.u.}$ and $Q_0 = -3e^2q/14I(2I-1)$, $a_0^3 = +0.896 \times 10^{-4} \text{ cm}^{-1}/\text{a.u.}$ for Cu^{63} . The quantity χ describes the contact interaction¹⁴ in the hfs, $\langle r^{-3} \rangle$ is the expectation value of r^{-3} in the t_2 configuration, and $\langle r^{-3} \rangle'$ is the matrix element of r^{-3} between the t_2 and e configuration. With two exceptions the expressions for the g factors and hfs constants are the same as those given by DKSY² when the following are used in (8):

$$\begin{aligned} a &= \frac{1}{3}\sqrt{3} (\cos\alpha + \sqrt{2} \sin\alpha), \\ b &= \frac{1}{3}\sqrt{3} (-\sqrt{2} \cos\alpha + \sin\alpha), \\ c &= -K'(2a + \sqrt{2}b)/(10Dq\sqrt{3}) + \sqrt{3}\zeta'b/(10Dq\sqrt{2}), \quad (9) \end{aligned}$$

where the second-order perturbation theory expression

¹² K. W. H. Stevens, Proc. Roy. Soc. (London) **A236**, 549 (1956).

¹³ D. Y. Smith, Phys. Rev. **137**, A574 (1965).

¹⁴ A. Abragam, J. Horowitz, and M. H. L. Pryce, Proc. Roy. Soc. (London) **A230**, 169 (1955).

for c is used and α , K' , and ζ' are as defined by DKSY. The latter two are the matrix elements of the axial crystal field and the spin-orbit interaction between the t_2 and e configurations. The exceptions are, first, that $g_{||}$ has an extra negative sign here, so that for a very strong axial field the spin-only value of $+2$ is obtained. Secondly, we obtain a different expression for the configuration interaction (CI) terms, which are the parts linear in c , in the hfs constants $A_{||}$ and A_{\perp} . This does not affect the fit obtained by DKSY appreciably because these terms contribute only about 1% of the total. However, more precise values of the $\text{ZnO}:\text{Cu}$ hfs constants¹⁵ do give different values for the net spin density χ . With the data of $A_{||} = -(198 \pm 3) \times 10^{-4} \text{ cm}^{-1}$ and $A_{\perp} = (224 \pm 1) \times 10^{-4} \text{ cm}^{-1}$, we obtain $\chi = -6.1 \pm 0.6 \text{ a.u.}$ and $\langle r^{-3} \rangle = 5.8 \pm 0.1 \text{ a.u.}$, compared with the free-ion values $\chi = -3 \text{ a.u.}$ ¹⁴ and $\langle r^{-3} \rangle = 8.25 \text{ a.u.}$, the latter computed from Hartree-Fock wave functions.¹⁶

The contents of Eq. (8) for the g factor may be displayed as a plot of $g_{||}$ versus g_{\perp} . This is shown in Fig. 3 for $c=0$, i.e., when the CI has been neglected. The effects of covalency appear as the different values of k which range from 1 to 0. The ratio a/b is varied and the values of $g_{||}$ and g_{\perp} are plotted. Tetrahedral symmetry corresponds to $a/b = \infty$ and the limits of strong axial fields correspond to $a/b = -\frac{1}{2}\sqrt{2}$ and $a/b = \sqrt{2}$. The allowed g factors are then found to be within the area bounded by the curves $k=1$, $k=0$, and $g_{\perp}=0$. When the CI is included it is possible to obtain combinations of $g_{||}$ and g_{\perp} which lie above the $k=1$ curve in this figure, except for T_d symmetry when the CI vanishes. A number of additional paramagnetic resonance observations of the $3d^9$ configuration¹ have been plotted in Fig. 3. One of these is the cubic Ni^+ spectrum in ZnS , two others are Ni^+ spectra with axial symmetry in ZnS . Other points are Cu in CdS ,

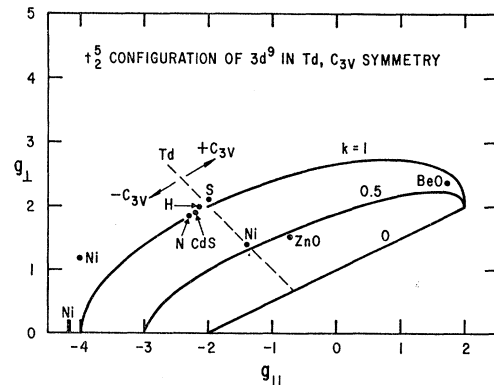


FIG. 3. Plot of $g_{||}$ versus g_{\perp} for the $3d^9$ configuration in C_{3v} symmetry for various orbital reduction factors k . The allowed g factors are bounded by the lines $k=1$, $k=0$, and $g_{\perp}=0$, when only the 2T_2 term is considered.

¹⁵ M. de Wit and T. L. Estle, Bull. Am. Phys. Soc. **8**, 24 (1963).

¹⁶ E. Clementi and A. D. McLean, Phys. Rev. **133**, A419 (1964); E. Clementi, IBM J. Res. Develop. Suppl. **9**, 2 (1965).

ZnO, and BeO. The three points labeled H, N, and S are three of the eight Cu spectra in ZnS. These points lie somewhat above the $k=1$ curve near T_d symmetry and could not be explained in terms of the present model. This is in contrast to the two axial Ni spectra which can be fitted, at least qualitatively.

An attempt to show that the observations in BeO may be fitted with Eq. (8) was made. For c the approximation in (9) was used. The unknown parameters in the five equations are then a/b , k , $\langle r^{-3} \rangle$, χ , N , $K'/10Dq$, and $\zeta'/10Dq$. We therefore make two further assumptions, first that $\zeta'/10Dq=0.14$, which corresponds to the free-ion value for ζ' with $10Dq=5700 \text{ cm}^{-1}$, the latter as observed in ZnO. The results are insensitive to this parameter, so that comparable quality fits were obtained with $\zeta'/10Dq=0.07$. Secondly, we satisfy Eq. (5) with $S=0.068$, compared with a value of 0.064 computed from the free-ion wave functions¹⁶ of Cu^{2+} and O^{2-} at the Be-O distance of 3.112 a.u. Equations (8) were then solved for the five remaining parameters, employing the nonlinear least-squares program of Marquardt¹⁷ modified so that weights can be included. The results are $a/b=-1.179$, $k=0.604$, $\langle r^{-3} \rangle=8.92 \text{ a.u.}$, $\chi=-2.89$, and $K'/10Dq=-0.248$, which yield $\eta=0.726$ and $N=0.867$. These results then indicate a large covalency effect with a hole density of 66% near the Cu nucleus and of 34% near the ligands. Furthermore, it is possible to explain the observations with physical quantities which are near the free-ion values. This is in contrast to the ZnO:Cu case, where we find that χ and $\langle r^{-3} \rangle$ are appreciably modified.

The dependence of the results on the overlap integral is such that for $S=0.056$ the results are $\chi=-3.00 \text{ a.u.}$ and $\langle r^{-3} \rangle=9.27 \text{ a.u.}$, with the other quantities within 0.3% of the values above. The observations then would seem consistent with the theory. However, a number of approximations had to be made and also the CI contribution is relatively large here. The CI is treated only to second order in perturbation theory and although it contributes 2% of the total of g_{\parallel} and 10% of g_{\perp} , the contributions to A_{\parallel} , A_{\perp} , and Q , respectively, 10, 30, and 1%, so that at least for A_{\perp} the approximation begins to break down.

SUMMARY

A crystal-field theory, which includes covalency effects, has been developed for the $3d^9$ configuration in C_{3v} by Dietz *et al.*² in connection with the center ZnO:Cu. This development is based on the effective Hamiltonian theory of Tanabe and Kamimura,¹¹ in which the structure of the Hamiltonian is determined by symmetry. Since the symmetry is low the number of parameters in the effective Hamiltonian is large and some simplifying assumptions had to be made in the treatment of the ZnO:Cu center. In the present application, a number of further simplifications have to be

¹⁷ D. W. Marquardt, *J. Soc. Indust. Appl. Math.* **11**, 431 (1963); IBM Share Program No. 1428 (unpublished).

made for the BeO:Cu center because we have only five experimentally measured quantities available, and these pertain to the ground state only. Therefore, we only attempted to show that the BeO:Cu observations are consistent with the above theory, but we are not able to provide support for the theory. The reason that the applicability of the theory to the $3d^9$ configuration might be questioned is the observation of some eight Cu centers in ZnS which have trigonal symmetry.¹ None of these centers are very well explained in terms of the theory. Although some of these centers must be associates of Cu with another defect and for some the paramagnetic electron is far removed from the Cu nucleus as evidenced by the small hyperfine interaction, no one is readily identified as the isolated substitutional Cu center with a $3d^9$ configuration. The $3d^9$ configuration of substitutional Ni in ZnS has also been observed.¹ The symmetry is cubic and the observations seem to fit the theory. However, there are now only three parameters available from experiment and even consistency with theory is difficult to show convincingly. An alternative interpretation for the center may be based on a dynamic Jahn-Teller effect. Briefly, the ground state of the substitutional Cu center is an orbital triplet and undergoes a tetragonal distortion so as to lower the total energy of the center and lattice. In addition, the various distortions are coupled so that a better description of the wave function is a linear combination of the various distorted functions. Some sort of association along the $\langle 111 \rangle$ directions has to be involved also in order to reproduce the observed symmetry for the ZnS:Cu centers but is not needed for the cubic ZnS:Ni center. The association model may be applicable to the wurtzite lattice where the axial part of the crystal field takes the place of association. The Jahn-Teller effect would have to override the spin-orbit interaction and the axial part of the crystal field, as has been observed in another system.¹⁸ In order to calculate the usual spin-Hamiltonian parameters from such a model, the Jahn-Teller effect for an electronic 2T_2 state would have to be known in considerable detail. Again, the number of parameters in the theory will be many more than five and physical arguments regarding the strength of various interactions such as we employed in order to simplify the theory of DKSY are not available for the much more poorly understood Jahn-Teller effect model.

ACKNOWLEDGMENTS

The authors are indebted to S. B. Austerman for graciously supplying the crystals used in this investigation, to D. R. Powell for performing the computer programming, and to Dr. T. L. Estle and Dr. W. C. Holton for numerous stimulating discussions.

¹⁸ T. L. Estle, G. K. Walters, and M. de Wit, in *Paramagnetic Resonance*, edited by W. Low (Academic Press Inc., New York, 1963), Vol. I, pp. 144-154; K. Morigaki, *J. Phys. Soc. Japan* **19**, 187 (1964).